Pure H_2 Production Through Hollow Fiber Hydrogen-Selective MFI Zeolite Membranes Using Steam as Sweep Gas

Yuting Zhang, Qi Sun, and Xuehong Gu
State Key Laboratory of Materials-Oriented Chemical Engineering, College of Chemistry and Chemical Engineering, Nanjing Tech University, Nanjing 210009, P.R. China

DOI 10.1002/aic.14924
Published online July 26, 2015 in Wiley Online Library (wileyonlinelibrary.com)

Hollow fiber MFI zeolite membranes were modified by catalytic cracking deposition of methyldiethoxysilane to enhance their H_2/CO_2 separation performance and further used in high temperature water gas shift membrane reactor. Steam was used as the sweep gas in the MR for the production of pure H_2. Extensive investigations were conducted on MR performance by variations of temperature, feed pressure, sweep steam flow rate, and steam-to-CO ratio. CO conversion was obviously enhanced in the MR as compared with conventional packed-bed reactor (PBR) due to the coupled effects of H_2 removal as well as counter-diffusion of sweep steam. Significant increment in CO conversion for MR vs. PBR was obtained at relatively low temperature and steam-to-CO ratio. A high H_2 permeate purity of 98.2% could be achieved in the MR swept by steam. Moreover, the MR exhibited an excellent long-term operating stability for 100 h in despite of the membrane quality. © 2015 American Institute of Chemical Engineers *AIChE J*, 61: 3459–3469, 2015
Keywords: hollow fiber, MFI zeolite membrane, membrane reactor, water gas shift reaction

Introduction

Hydrogen energy has attracted worldwide attention in last decades for its combined advantages of high energy transferring efficiency and zero pollution emission. Water gas shift (WGS, $CO+H_2O \leftrightarrow CO_2+H_2$, $\Delta H = -41.4$ kJ mol^{-1}) reaction is a critical process for H_2 production from fossil fuels or biofuels. The reaction is reversible and exothermic, thus it requires a two-step operation including high temperature shift (HT-WGS, 300–450°C) and low temperature shift (LT-WGS, 150–300°C) to achieve high reaction rate and deep conversion. However, this process has some drawbacks such as complex operating, large catalyst volumes and high steam recycling.[1,2] Recently, a membrane reactor (MR) integrating the reaction with product separation using a hydrogen-selective membrane has been considered as an alternative strategy to optimize the process. The WGS MR exhibits great potential to fulfill one-step operation for deep CO conversion by immediate removal of hydrogen from reaction system.[3–7]

In the last two decades, a couple of hydrogen-separating membranes have been investigated for WGS reaction. Pd-based MRs[3,4] have been widely considered because H_2 selectivity of Pd-membrane is extremely high. However, it would be hardly to spread the application of Pd-based membrane in large scale due to high cost of palladium. Compared to Pd-based dense membrane, microporous ceramic membranes provide advantages of relatively low cost and good tolerance for H_2S and CO. Silica membranes have been found to exhibit high selectivity for separation of H_2/CO_2 mixture.[6–9] But the improvement of hydrothermal stability at HT is still a challenge for the membranes to be applied in practical WGS reaction system. Crystalline MFI zeolite membranes, possessing excellent thermal and chemical stabilities, have been studied for hydrogen separation in recent years.[10–16] As the zeolitic pore size (~0.55 nm) is larger than both kinetic diameters of H_2 (~0.29 nm) and CO_2 (~0.33 nm), pore modification was performed to fit H_2/CO_2 separation. Masuda et al.[10] proposed a catalytic cracking of silane method by preloading silane in zeolite channels at saturation level and then decomposing it at 550°C in air. A significant increase in H_2/N_2 separation factor up to 100 was obtained after the modification. However, a large reduction in H_2 permeance was found at the same time due to the excessive deposition of SiO_2. To avoid excessive deposition, we proposed an on-stream modification for MFI zeolite membrane by catalytic cracking deposition (CCD) of methyldiethoxysilane (MDES).[11] H^+ ion exchange on MFI/α-Al_2O_3 membranes was used to provide more active sites for CCD, which produced a modified MFI zeolite membrane with a H_2/CO_2 separation factor of 42.1 at 500°C.[16] We further modified hollow fiber type MFI zeolite membranes which provided high packing density (>800 m^2 m^{-3}) and low fabrication cost. They also showed an excellent H_2/CO_2 separation performance and good tolerances under steam and H_2S atmospheres,[17] which seemed more suitable for WGS reaction considering the practical application in the future. In our previous work, a hydrogen-separating MFI zeolite membrane packed with $CuO/ZnO/Al_2O_3$ catalysts was applied in LT WGS MR, showing an obvious increment in conversion compared to a conventional packed bed reactor (PBR).[18]

Until now, most researchers used inert gases (such as He and N_2) to sweep the permeated hydrogen in WGS MRs. Therefore, a secondary separation is required to obtain pure

Correspondence concerning this article should be addressed to X. Gu at xhgu@njtech.edu.cn.

hydrogen. Evacuation by pump is an alternative to the sweeping operation, but it means high energy consumption. In this work, steam was first used as sweep gas in hollow fiber MFI zeolite MR for pure H_2 production through HT-WGS membrane reaction. Extensive investigations on the membrane separation as well as the catalytic process were performed for better understanding the integration process and H_2 permeate purity. Long-term stability of the tested membranes in the WGS reaction was also investigated to evaluate the feasibility of the process for practical application in the future.

Experimental

Membrane preparation and modification

MFI zeolite membranes were prepared on α-Al_2O_3 hollow fiber supports by *in situ* crystallization. The hollow fiber supports had I.D./O.D. of about 1.8 mm/0.8 mm, an average pore size of 500–600 nm and porosity of 31–33%. The synthesis precursor was prepared by mixing sodium hydroxide (99.99%, Aldrich), tetrapropylammonium hydroxide solution (TPAOH, 1M, Aldrich), fumed SiO_2 (99.98%, Aldrich) and deionized water at 80°C. The molar composition for the synthesis solution was $1(TPA)_2O$: $6.66SiO_2$: $0.35Na_2O$: $92.2H_2O$. Hydrothermal crystallization was carried out at 180°C for 5 h. The synthesized membranes were calcined in air at 450°C for 8 h for template removal.

For modification, a hollow fiber MFI zeolite membrane was mounted in a stainless steel cell. An equimolar H_2/CO_2 feed gas (40 mL min^{-1}) mixed with helium stream (5 mL min^{-1}) carrying MDES (Alfa Aesar) vapor (0.72 kPa) was introduced to membrane side of hollow fiber membrane, while another helium stream with a flow rate of 30 mL min^{-1} was used to sweep the support side. CCD of MDES was operated at 500°C for 1–2 h and both sides were controlled at atmospheric pressure. Detailed synthesis procedure and modification for hollow fiber MFI zeolite membranes can be found in our previous publication.[17]

The permeance P_m (mol m^{-2} s^{-1} Pa^{-1}) through zeolite membrane was calculated by

$$P_m = J/\Delta p \tag{1}$$

where J is permeation flux through membrane, mol m^{-2} s^{-1}; Δp is the partial pressure difference between both sides of the membrane, Pa.

The ideal selectivity ($S_{i/j}$) for component i over j is calculated from the single gas permeances of i ($P_{m,i}$) and j ($P_{m,j}$) by

$$S_{i/j} = P_{m,i}/P_{m,j} \tag{2}$$

The separation factor ($\alpha_{i/j}$) for component i over j is given by

$$\alpha_{i/j} = \frac{(y_i/y_j)_{\text{permeate}}}{(y_i/y_j)_{\text{retentate}}} \tag{3}$$

where y_i and y_j are, respectively, mole fraction of i and j for permeate or retentate.

It has been reported that the permeance of a nonadsorbing or weak adsorbing small gas molecules through MFI zeolite membranes can be described by the following equation[19]

$$P_{m,i} = \frac{\varphi\delta}{Lz}\left(\frac{8}{\pi M_i RT}\right)^{0.5}\exp\left(\frac{-E_d}{RT}\right) \tag{4}$$

where $P_{m,i}$ is the single gas permeance (mol m^{-2} s^{-1} Pa^{-1}), R is the gas constant (J mol^{-1} K^{-1}), L is the thickness of the zeolite membrane layer (m), T is the temperature in kelvin (K), E_d is the activation energy for gas permeance through the MFI zeolite membrane (J mol^{-1}), φ is the ratio of the membrane porosity to tortuosity, M_i is the molecular weight of the permeating gas (g mol^{-1}), δ is about 1 nm for diffusion in a MFI-type zeolite, and z is the diffusion coordination number (4 for a MFI-type zeolite).

Membrane reaction

Figure 1 shows schematic diagram of the experimental apparatus for HT-WGS membrane reaction. A modified hollow fiber MFI zeolite membrane was mounted in a stainless steel reactor and put in a furnace. The membrane had an effective length of 6 cm with active membrane area of 3.4 cm^2. One end of the membrane was sealed by high temperature glue (HT2712, Huitian New material Co.) and the other end was connected to permeate side. 0.5 g commercial Fe_2O_3/Cr_2O_3/Al_2O_3 catalyst (20–40 mesh, BET area: 88.12 cm^2 g^{-1}, Nanjing Catalysts Company) was packed in the shell side of MR, which was fed with a gas mixture of 33.3%CO/66.7%H_2 and preheated steam. A glass capillary tube was inset into the lumen of the hollow fiber for introducing sweep gas. When using steam as sweep gas, the steam gas was generated from liquid water plugged by a micro pump (2ZB-1L10, Beijing Weixing) and then preheated via heat-exchange with the hot downstream from the MR. Both gas flow rates of N_2 and steam was varied between 0–25 mL min^{-1}. The feed side was controlled at an absolute pressure between 0.1–0.15 MPa while the permeate side was maintained at atmospheric pressure. The WGS reaction was operated at 300–450°C. After dehumidification by a water trapper, the reaction products were analyzed by a gas chromatograph (GC-2014, Shimadzu) equipped with a thermal conductivity detector and a packed column of Hayesep DB (Alltech). Methane (20 mL min^{-1}) was used as an internal standard for composition analysis. The CO conversion (χ_{CO}) for WGS reaction was calculated by Eq. 5 on basis of the CO feed flow rate ($F_{CO,in}$, mol s^{-1}) and the molar rates of CO in permeate side ($F_{CO,p}$, mol s^{-1}) and retentate side ($F_{CO,r}$, mol s^{-1}); the H_2 recovery (R_{H_2}) for MR was calculated by Eq. 6 based on the flow rate of H_2 in retentate side ($F_{H_2,r}$, mol s^{-1}) and the molar rate of H_2 in permeate side ($F_{H_2,p}$, mol s^{-1}); the H_2 purity (P_{H_2}) in the permeate side was calculated by Eq. 7 based on the permeated H_2, CO, and CO_2 flow rates ($F_{H_2,p}$, $F_{CO,p}$, and $F_{CO2,p}$, mol s^{-1})

$$\chi_{CO} = \left(1 - \frac{F_{CO,p}+F_{CO,r}}{F_{CO,in}}\right)\times 100\% \tag{5}$$

$$R_{H_2} = \frac{F_{H_2,p}}{F_{H_2,p}+F_{H_2,r}}\times 100\% \tag{6}$$

$$P_{H_2} = \frac{F_{H_2,p}}{F_{H_2,p}+F_{CO,p}+F_{CO_2,p}}\times 100\% \tag{7}$$

Kinetic Equation. The equilibrium CO conversion ($\chi_{CO,e}$) was determined by equilibrium constant (K_e) based on the following equation

$$\frac{\chi_{CO,e}(2+\chi_{CO,e})}{(1-\chi_{CO,e})(R_{H_2O/CO}-\chi_{CO,e})} = K_e \tag{8}$$

where $R_{H_2O/CO}$ is feed steam-to-CO ratio and K_e is given by[20,21]

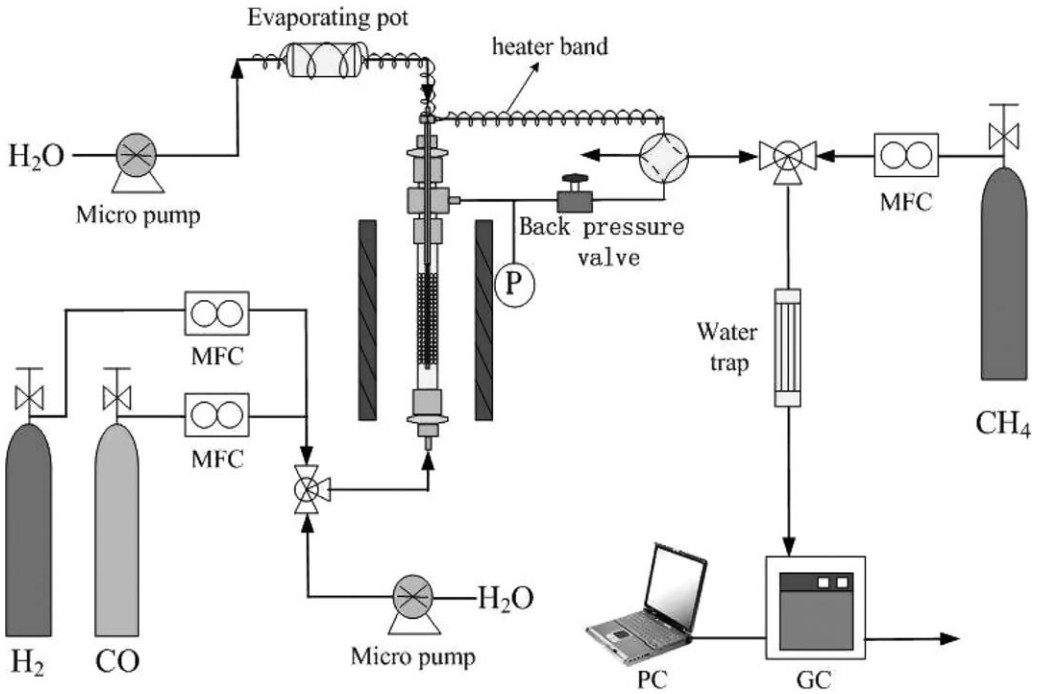

Figure 1. Schematic diagram of hollow fiber MFI zeolite membrane reactor for HT-WGS reaction swept by steam.

$$K_e = \exp\left(\frac{4577.8}{T} - 4.33\right) \tag{9}$$

The WGS kinetic rate equations on basis of the Power Law equation[21] were simulated and solved numerically via standard fourth order Runga–Kutta algorithm using Visual C++ 6.0 software

$$-\Re_{CO} = -10^{-3.88}\exp\left(-\frac{64063.5}{RT}\right)p_{CO}^{0.9}p_{H_2O}^{0.5}p_{H_2}^{-0.6}\left(1-\frac{p_{CO_2}p_{H_2}}{K_e p_{CO}p_{H_2O}}\right) \tag{10}$$

$$K_e = \left(\frac{p_{CO_2}p_{H_2}}{p_{CO}p_{H_2O}}\right)_e \tag{11}$$

where $\Re_{CO}$ is the reaction rate (mol g_{cat}^{-1} s^{-1}); K_e is the WGS reaction equilibrium constant calculated by Eq. 9; p_i is the partial pressure of component i; R is the gas constant (8.314 J mol^{-1} K^{-1}), T is the temperature in kelvin (K).

Membrane Reaction Model. The hollow fiber MR in this study was described as a simple one dimension plug-flow reactor.[22] Some assumptions were considered: (1) isothermal steady-state operation; (2) no side reactions; (3) negligible pressure drops across the retentate and permeate; and (4) ideal gas behavior.

The membrane reaction is described by the following mass balance equation

$$\text{Feed side}: \frac{dF_i}{dl} = \frac{1}{4}\pi(D^2-d^2)\rho_{cat}\nu_i\Re_i - \pi d P_{m,i}\Delta p_i \tag{12}$$

$$\text{Permeate side}: \frac{dQ_i}{dl} = \pi d P_{m,i}\Delta p_i \tag{13}$$

where F_i and Q_i are the molar flow rate on the feed and permeate sides, respectively (mol s^{-1}); l is the reactor length (m); D and d are the inner diameter of the reactor tube and outer diameter of the hollow fiber membrane, respectively (m); ρ_{cat} is the packing density of the $Fe_2O_3/Cr_2O_3/Al_2O_3$ catalyst (6.5×10^5 g_{cat} m^{-3}); ν_i is the stoichiometric coefficient; $P_{m,i}$ represents the gas permeance of specie i under specific experimental operation; Δp_i is the partial pressure difference of specie i between the feed side and permeate side (Pa).

Result and Discussion

Gas permeation

Figure 2 shows SEM images of a hollow fiber MFI zeolite membrane before and after CCD modification. A well-intergrown zeolite film with a thickness of 4 μm was formed on the outer surface of hollow fiber substrate (Figures 2a, b). No obvious difference was found on the morphology of membrane surface before and after modification (Figures 2c, d). N_2 and steam were separately used as sweep gas to test H_2, CO_2, and CO single gas permeations for comparison. The sweep gas flow rate was controlled at 25 mL min^{-1}. Figure 3 illustrates single gas permeation results of two modified membranes (M1 and M2) swept by N_2 and steam at different temperatures. We can see that H_2 permeance increased gradually with the temperature in a manner of activated diffusion although the membranes had different H_2 selectivities. On basis of Eq. 4, the calculated activated diffusion energies of M1 and M2 were 6.89 and 6.91 kJ mol^{-1}, respectively. The similar result could be owed to their similar membrane configuration. Conversely, the permeances of larger molecules (CO and CO_2) decreased initially and then climbed up with the elevated temperature. This phenomenon implied that the dominant permeation mechanism for CO and CO_2 changed from surface diffusion at lower temperature to activated diffusion at higher temperature.[19] Although having lower H_2 permeance, M2 offered a higher H_2/CO_2 permselectivity than M1. When using N_2 as sweep gas, M2 had a H_2/CO_2 permselectivity of 36.9 while M1 had a value of 9.7 at 450°C. The result implied that M2

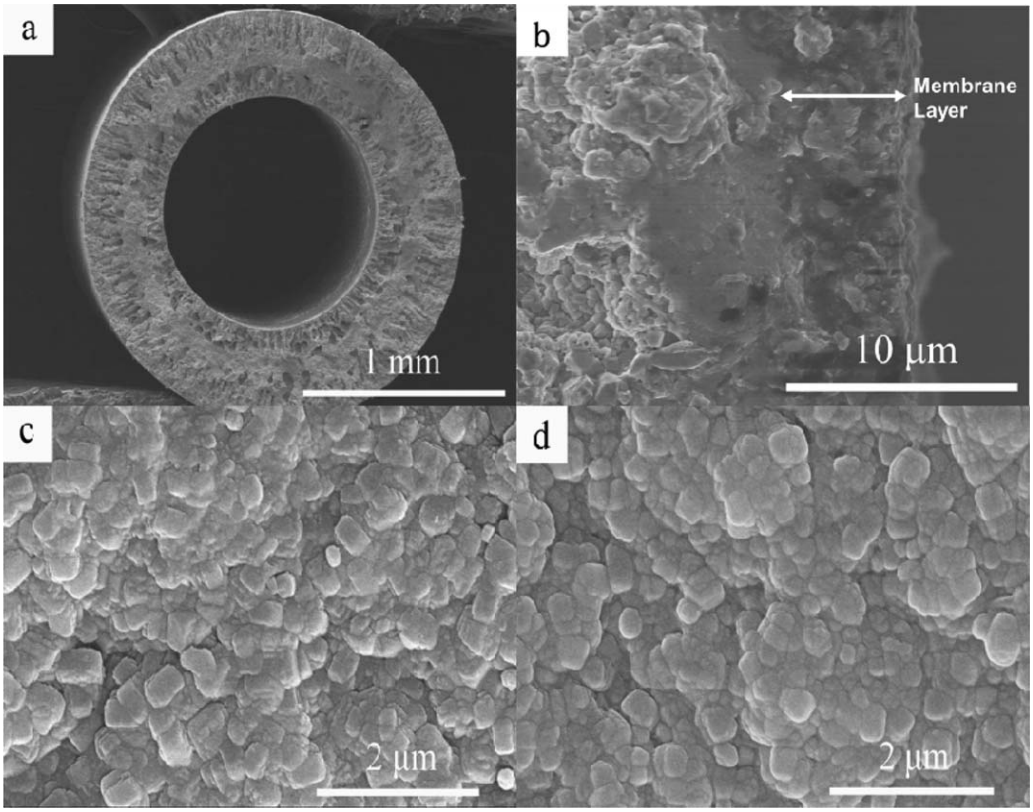

Figure 2. SEM images of the hollow fiber MFI zeolite membranes: (a) and (b) cross section; membrane surface (c) before and (d) after modification.

had a better quality for MFI zeolite membrane layer, which was helpful for modification. Moreover, the minimum permeances of CO_2 and CO curves for M2 were observed at lower temperature compared to M1, suggesting that M2 had less amount of small intercrystalline defects. Similar phenomenon was found by Zhu et al.,[13] who investigated the effect of membrane quality on modification performance. They suggested that the MFI zeolite membrane with fewer defects could be effective for enhancing H_2/CO_2 separation factor. When using steam as sweep gas, we found decreases in permeances for all the three gases (H_2, CO, and CO_2). Tang et al.[23] suggested that gas permeation through modified MFI zeolite membrane could be inhibited by the counter-diffusion of sweep gas from the opposite side of the membrane. As a small and strong absorbing molecule, H_2O was thought to bond on Si—OH groups which existed in MFI zeolite channel surfaces at LT.[24] However, when the temperature was high enough (especially above 300°C) that the absorbing capacity of H_2O in zeolite channels decreased and even disappeared, H_2O would appear a strong temperature-sensitive activated diffusion due to its high permeation diffusivity and low activated diffusion energy as related to its small diameter size (0.28 nm) and light molecule mass.[19,25] The steam sweep gas diffusing back through membrane pores was considered to make a hindrance for other gas permeation. The extent of reduction in gas permeance caused by steam sweep gas increased with the molecule size of permeating gases (i.e., the gas permeance of M2 swept by steam was about 45.4, 32.2, and 18.5% of that swept by N_2 for H_2, CO_2, and CO, respectively). Namely, the steam sweep gas led to increases in H_2 permselectivities for the membrane. At 450°C, M1 had a H_2/CO_2 and H_2/CO permselectivities of 10.3 and 12 while M2 had values of 52 and 78.8. The difference between the increases in H_2 permselectivities for the membranes could be explained by that the hindrance effect caused by steam was more prominent in narrow pores (such as zeolitic pore) rather than larger pores (such as small intercrystalline defect). Namely, it hindered gas permeations more significantly for the membrane with better quality.

Membrane reaction

Effect of Composition of N_2-Steam Mixed Sweep Gas. The membranes M1 and M2 were used in HT-WGS reaction with 0.5 g $Fe_2O_3/Cr_2O_3/Al_2O_3$ catalyst loading for H_2 production. The reactions were operated at temperatures ranging from 300 to 450°C and the permeate side was kept at atmospheric pressure. The membrane reaction was first carried out using a N_2-steam binary mixed gas as sweep gas. The steam content of the sweep gas mixture was varied by changing the liquid water flow rate meanwhile the total sweep gas flow rate was maintained at 25 mL min^{-1} constantly. The gas hourly space velocity (GHSV) and feed steam to CO ratio ($R_{H_2O/CO}$) was fixed at 1800 $L_N\ g_{cat}{}^{-1}h^{-1}$ and 1.25, respectively. As shown in Figure 4, M1 provided a higher χ_{CO} than M2 under the same condition due to its higher H_2 permeance and thus larger amount of H_2 removal from the reaction system. When using pure steam as sweep gas, the CO conversions in M1 and M2 (73.6 and 70.9%) were a little lower than those swept by pure N_2 (76.1 and 73.1%) but also noticeably higher than the CO conversion in PBR (63.4%). As shown in Figure 5, the sweeping steam not only removed H_2 from the reaction system but also brought in a counter-diffusion toward the reaction side. Both effects were positive for improving the reaction kinetic. We also noted that the steam diffusion made a hindrance effect on the H_2 permeation at the same time, which resulted in a less

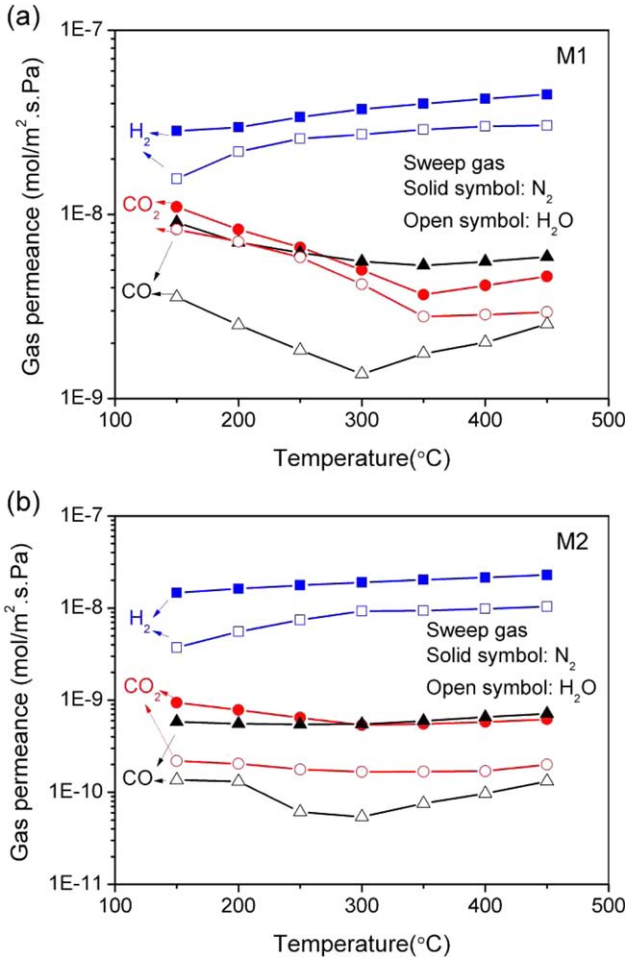

Figure 3. Single gas permeation tests swept by N_2 and steam for the membranes: (a) M1 and (b) M2.

[Color figure can be viewed in the online issue, which is available at wileyonlinelibrary.com.]

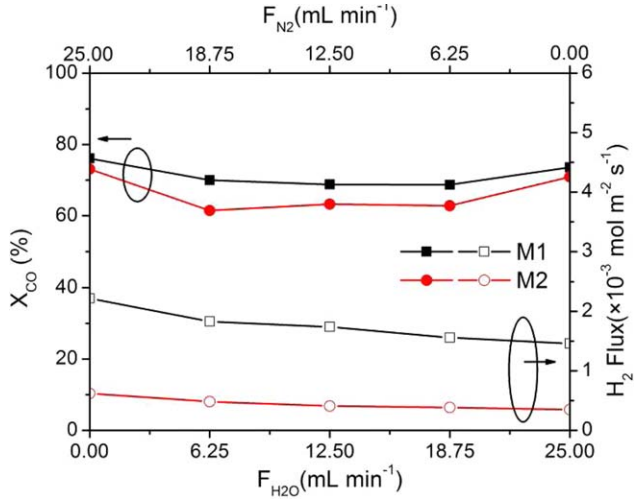

Figure 4. Effect of steam content of the N_2-steam binary sweep gas mixture on CO conversion and H_2 flux for HT-WGS in the membrane reactor (operating conditions: T=350°C, GHSV=1800 L_N kg_{cat}^{-1} h^{-1}, $R_{H_2O/CO}$=1.25).

[Color figure can be viewed in the online issue, which is available at wileyonlinelibrary.com.]

increment in conversion. It was interesting to find that although the membrane had higher H_2 permeate flux, the conversion for sweeping by N_2-steam mixed gas was lower than that for sweeping by pure steam. This phenomenon can be explained by that the steam partial pressure in the sweep side was diluted by N_2 and the H_2O counter-diffusion was weakened due to the lowered steam driving force through the membrane. It demonstrated that sweeping with pure steam was helpful for enhancing the conversion and acquiring the pure H_2 product directly. Our further studies were focused on using pure steam as sweep gas.

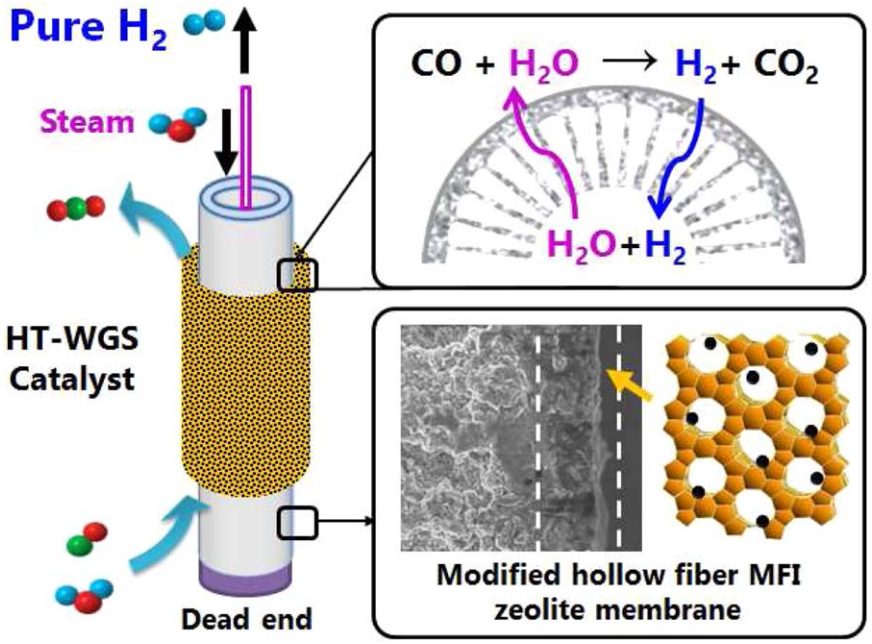

Figure 5. Schematic illustration of WGS membrane reactor with hollow fiber MFI zeolite membrane swept by steam.

[Color figure can be viewed in the online issue, which is available at wileyonlinelibrary.com.]

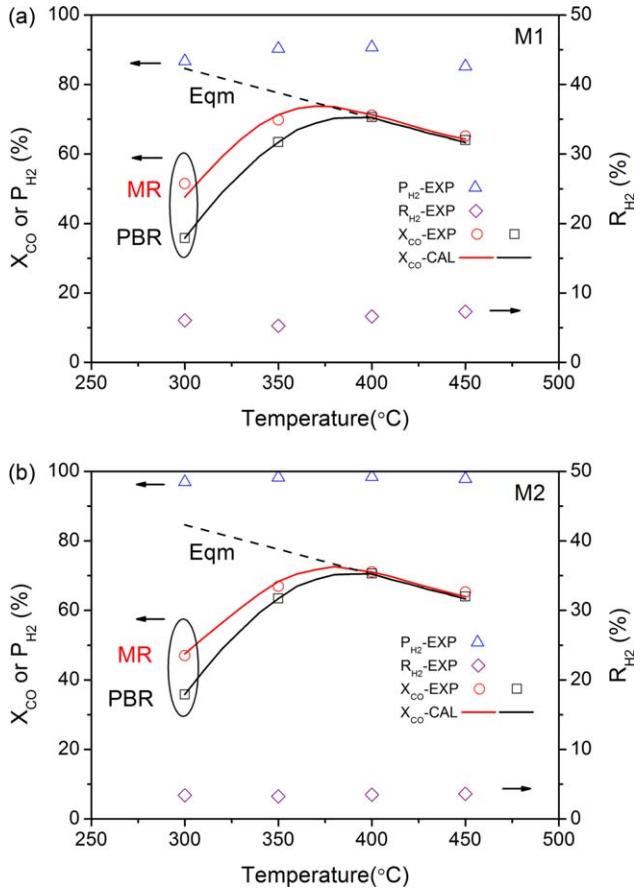

Figure 6. Temperature dependence of CO conversion, H_2 recovery and permeate purity for the HT-WGS MR using M1 (a) and M2 (b) (operating conditions: GHSV=1800 L_N kg_{cat}^{-1} h^{-1}, R_{H_2O}= 1.25, F_{H_2O}= 6.25 mL min^{-1}).

[Color figure can be viewed in the online issue, which is available at wileyonlinelibrary.com.]

Effect of Reaction Temperature. In comparison with MR, we investigated a conventional packed-bed reactor (PBR) using the similar feed conditions. As shown in Figure 6, both M1 and M2 exhibited higher CO conversions than PBR, especially at LT. As the temperature increased, both conversions in PBR and MR increased initially due to the improved kinetic rate and then declined due to the thermodynamic limit. At 400°C, the maximum conversions for M1 and M2 were achieved to be 71.2 and 71.1%, respectively, while the conversion in PBR was 70.6%. For M1, the increment in χ_{CO} for MR vs. PBR decreased from 15.7 to 1.2% as the temperature increased from 300 to 450°C. The result implied that reaction equilibrium could be a key factor for the reaction system to affect the conversion increment.[26] At LT, the kinetic-limiting conversion was markedly enhanced by H_2 removal from the reaction system and H_2O counter-diffusion from the permeate side. However, when come to HT where the conversion was limited by the equilibrium, slight variation took place in the conversion due to the thermodynamic state which was related to the feed flow composition.[18] When the temperature climbed up from 300 to 450°C, the R_{H_2} for M1 increased from 6.1 to 7.3% while M2 increased slightly from 3.4 to 3.6%. We also noted that the dependency of P_{H_2} as a function of temperature was similar to the trend of CO conversion. The increase in P_{H_2} at lower temperatures was attributed to the increase of H_2 separation selectivity with temperature. It was not clear that the further decrease in P_{H_2} when the temperature was further increased. Smart et al.[27] found that the H_2 permeate purity for microporous silica membrane increased with the feed H_2 concentration in H_2/CO_2 gas mixture. We speculated that the further decline in conversion from 400 to 450°C resulted in a reduction in H_2 partial pressure and increases in CO_2 and CO partial pressures in the retentate side, which were considered to be negative for the H_2 permeate purity.

Effect of Feed Pressure. As WGS reaction has no variation of mole number, the equilibrium conversion is independent of the reaction pressure in PBR.[28] However, high H_2 pressure drop through the membrane is in favor of H_2 permeation in MR, which is helpful for CO conversion. One method to achieve this is to increase the feed pressure. From mechanical viewpoint, it is noteworthy that the pressure gradient between the lumen and shell side of the ceramic hollow fiber membrane should not be very high to avoid membrane breaking. We investigated the CO conversion, H_2 recovery and H_2 permeate purity under a feed pressure of 0.15 MPa (absolute pressure) in comparison with atmospheric pressure while the GHSV, $R_{H_2O/CO}$ and sweep steam flow rate (F_{H_2O}) was fixed at 1800 L_N g_{cat}^{-1} h^{-1} and 1.25, respectively. As shown in Figure 7, R_{H_2} was noticeably enhanced at higher feed pressure due to the enlarged

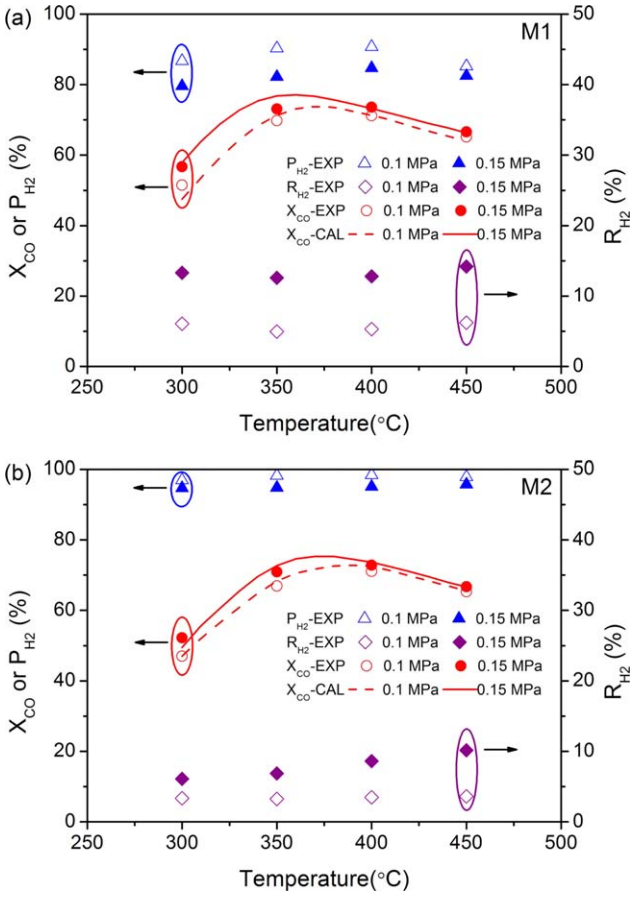

Figure 7. Effect of feed pressure on CO conversion, H_2 recovery and permeate purity for the HT-WGS MR using M1 (a) and M2 (b) (operating conditions: R_{H_2O}=1.25, GHSV =1800 L_N kg_{cat}^{-1} h^{-1}, F_{H_2O}=6.25 mL min^{-1}).

[Color figure can be viewed in the online issue, which is available at wileyonlinelibrary.com.]

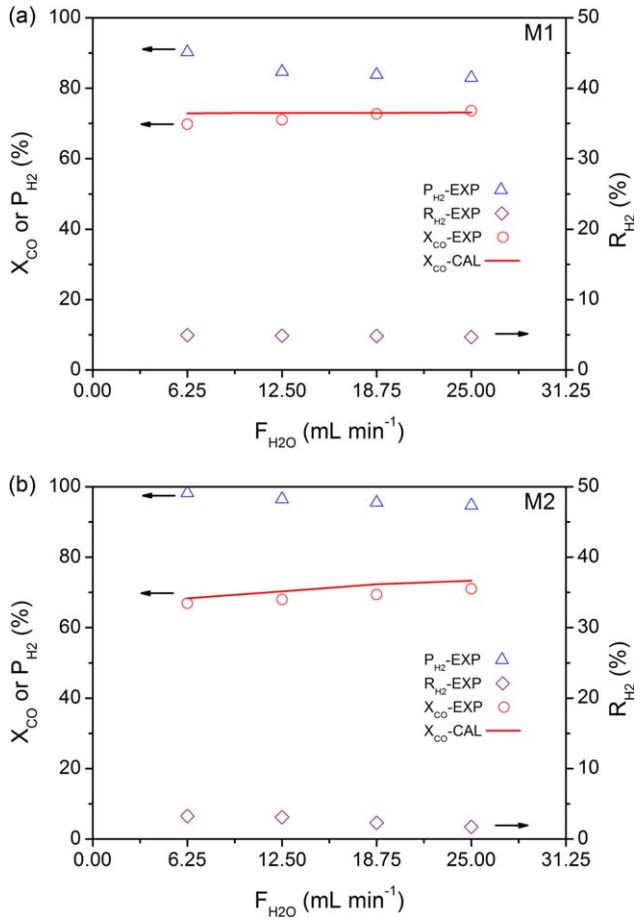

Figure 8. Effect of sweep steam flow rate on CO conversion, H_2 recovery and permeate purity for the HT-WGS MR using M1 (a) and M2 (b) (operating conditions: T=350°C, GHSV=1800 L_N $kg_{cat}^{-1}h^{-1}$, $R_{H_2O/CO}$=1.25).

[Color figure can be viewed in the online issue, which is available at wileyonlinelibrary.com.]

H_2 pressure drop through the membrane which promoted the H_2 permeation. Owing to the enhanced amount of H_2 removal from the reaction system, high feed pressure was effective for enhancing the conversion, especially at LT. We also noted that the both increments in conversions for M1 and M2 were very slight at 450°C. It seemed that the feed pressure significantly influenced the reaction kinetic but made a slight effect on the equilibrium state. Similar phenomenon was also observed by Kim et al.,[28] who carried out a disk-shaped MFI membrane for WGS reaction and found a slight increment in CO conversion by increasing the feed pressure. Moreover, an increase in feed pressure also resulted in enlargement of the inlet steam partial pressure in the feed side. The H_2O counter-diffusion toward the reaction system was weakened for the reduction of driving force through the membrane. Conversely, the P_{H_2} was found to decrease with the feed pressure. The decrease was more significant for M1 as compared with M2. This could be due to that more components from reaction system permeated unselectively through intercrytalline defects of membrane layers at higher feed pressure.

Effect of Sweep Steam Flow Rate. Other methods for increasing H_2 pressure drop are decreasing the permeate chamber pressure by vacuum mode or sweep gas. Vacuum

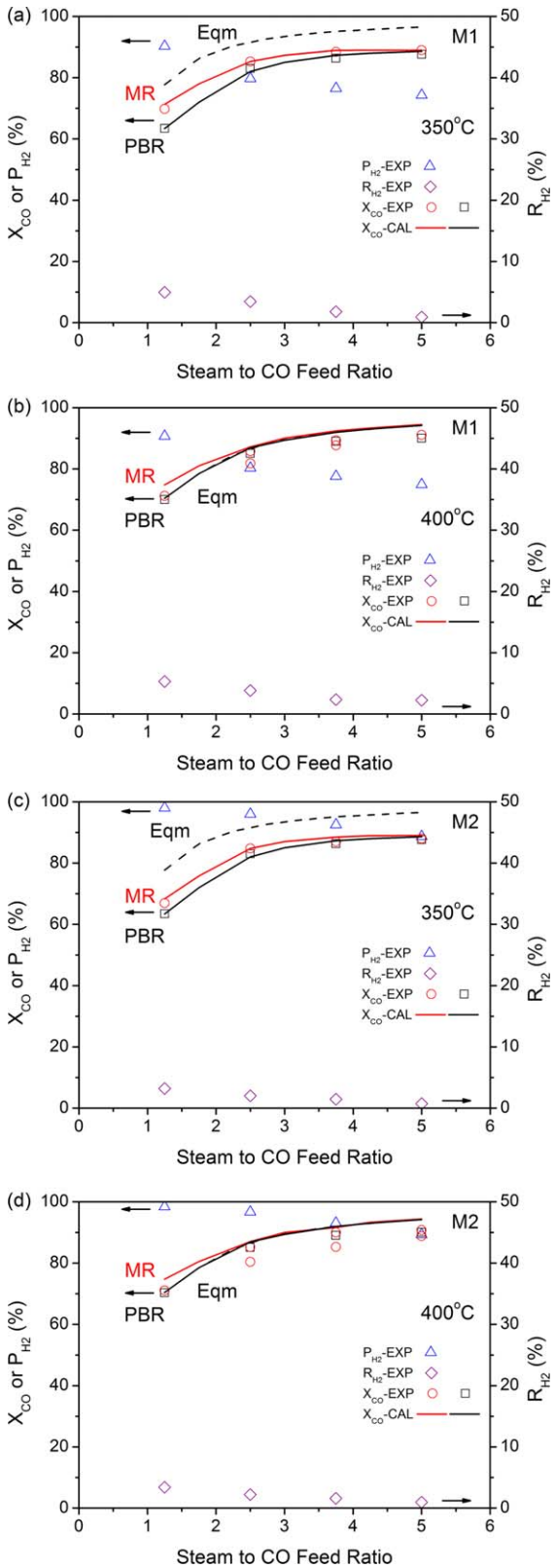

Figure 9. Effect of Steam to CO feed ratio on CO conversion, H_2 recovery and permeate purity for the HT-WGS MR using M1 (a and b) and M2 (c and d) (operating conditions: GHSV=1800 L_N kg_{cat}^{-1} h^{-1}, F_{H_2O}=6.25 mL min^{-1}).

[Color figure can be viewed in the online issue, which is available at wileyonlinelibrary.com.]

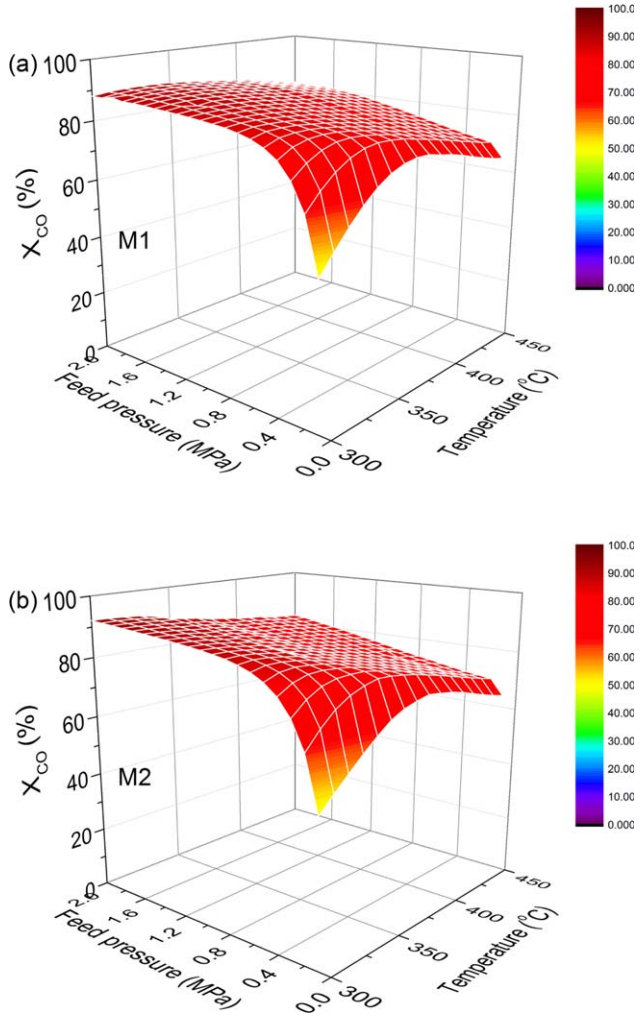

Figure 10. Calculated CO conversion in MR for M1 (a) and M2 (b) as a function of temperature and feed pressure (operating conditions: GHSV=1800 L_N kg_{cat}^{-1} h^{-1}, F_{H_2O}=6.25 mL min^{-1}, $R_{H_2O/CO}$=1.25).

[Color figure can be viewed in the online issue, which is available at wileyonlinelibrary.com.]

mode is not encouraged for its high energy consumption. The sweep steam flow could dilute the H_2 partial pressure in the permeate side and thus promote the H_2 removal from the reaction system. Figure 8 shows the effect of sweep steam flow rate on CO conversion, H_2 recovery and H_2 permeate purity in MR. The reactions were conducted under GHSV=1800 L_N $g_{cat}^{-1}h^{-1}$ and $R_{H_2O/CO}$=1.25. As expected, M1 offered a higher conversion than M2. But M2 had a better P_{H_2} than M1 due to its better H_2 separation selectivity. When the sweep steam flow rate was 6.25 mL min^{-1}, M2 exhibited a high H_2 permeate purity of 98.2% while its CO conversion was 66.9%. By contrast, M1 showed a lower P_{H_2} of 90.3% and a little higher χ_{CO} of 69.8%. It can be also seen from the figure that the sweep steam flow rate made a negative effect on H_2 recovery, falls of less than 0.5% and about 1.5% in R_{H_2} occurred for M1 and M2, respectively. We suggest that high sweep steam flow rate on one hand brought about reduction in permeated H_2 partial pressure but on the other hand led to increase in steam partial pressure in the permeate side, which resulted in a counter-diffusion of steam that had a suppressive effect on H_2 permeation. It is noteworthy that the P_{H_2} also decreased with the sweep steam flow rate. When the sweep steam flow rate climbed from 6.25 up to 25 mL min^{-1}, falls of 7.3% and 3.5% occurred in the P_{H_2} for M1 and M2, respectively. As similar with increasing feed pressure, such declining behavior of P_{H_2} was followed by the enhanced permeations through the non-zeolitic pores. To achieve high H_2 permeate purity, the sweep steam flow rate was controlled at 6.25 mL min^{-1} in the further study.

Effect of Steam-to-CO Feed Ratio. It is well known that R_{H_2O}/CO could influence the reaction rate, equilibrium conversion and H_2O pressure drop through the membrane in WGS MR. High steam to CO ratio favors high CO conversion in PBR but it also demands a lot of vaporization heat. Here, we investigated the effect of $R_{H_2O/CO}$ on CO conversion, H_2 recovery and H_2 permeate purity for MR at 350 and 400°C. As shown in Figure 9, the R_{H_2} decreased continuously with the $R_{H_2O/CO}$. It can be explained that although high steam/CO ratio forwarded the reaction and generated more amount of hydrogen, the H_2 partial pressure in the feed side decreased

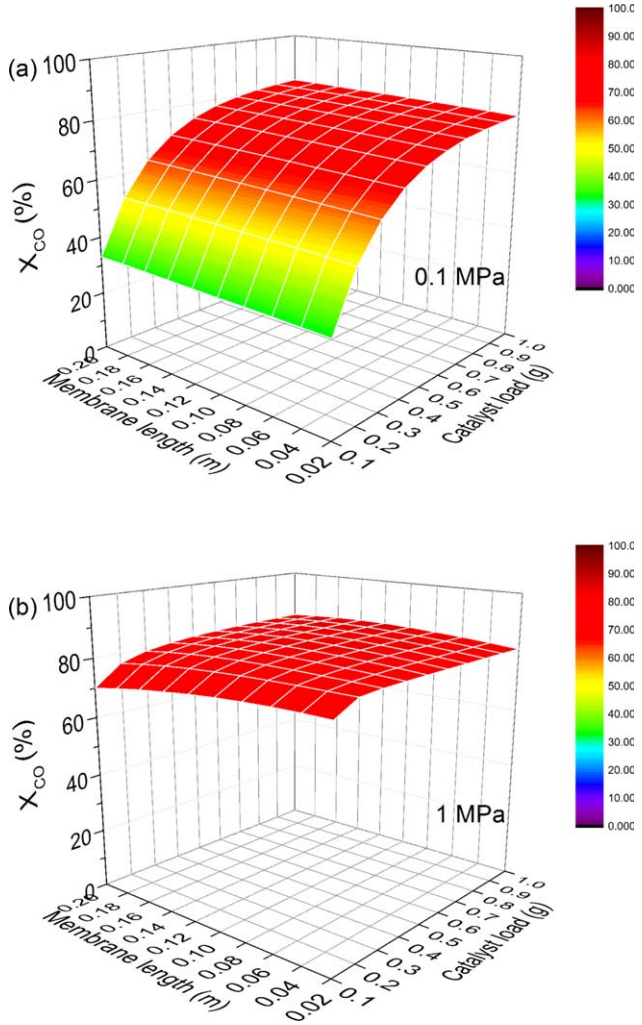

Figure 11. Calculated CO conversion in MR for M1 as a function of membrane length and catalyst load under feed pressure of 0.1 MPa (a) and 1 MPa (b) (operating conditions: T=350°C, F_{H_2O}=6.25 mL min^{-1}, $R_{H_2O/CO}$=1.25).

[Color figure can be viewed in the online issue, which is available at wileyonlinelibrary.com.]

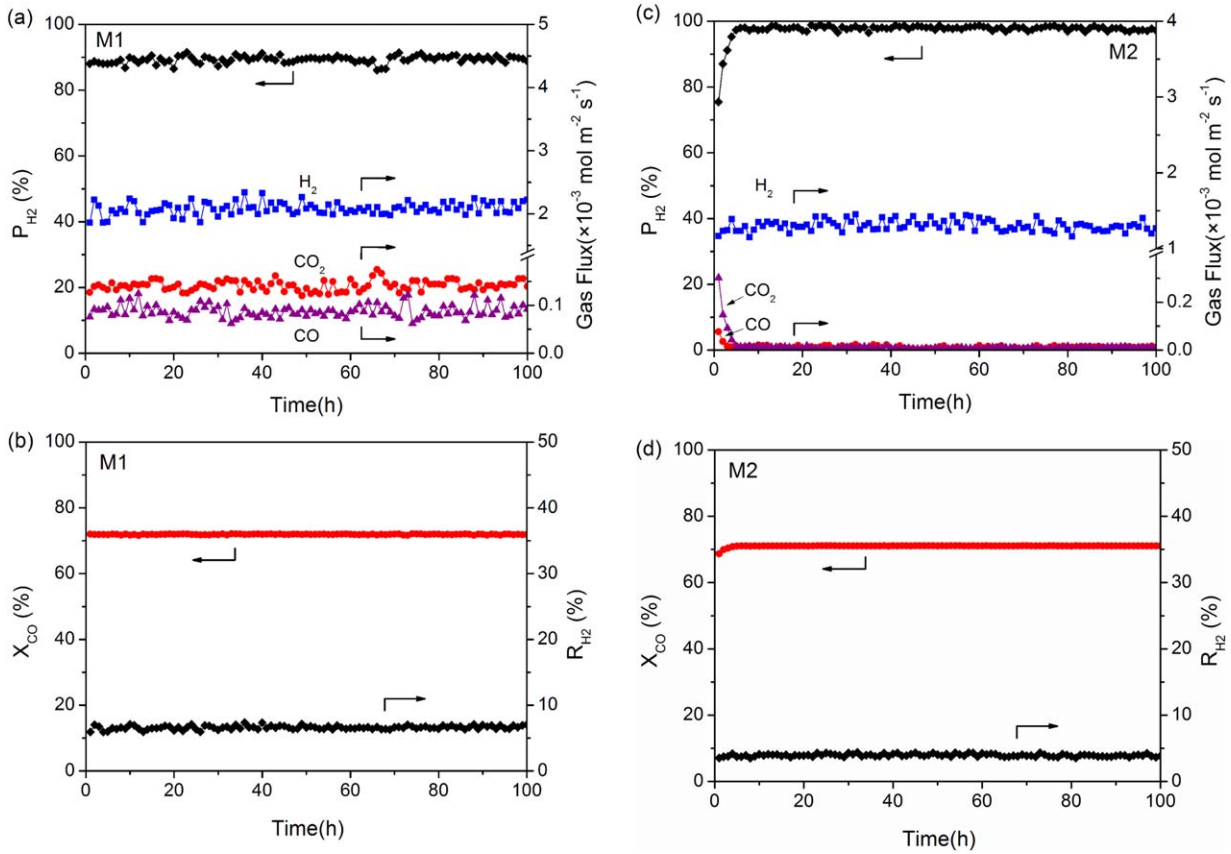

Figure 12. Long term stability in HT-WGS reaction for the modified hollow fiber MFI zeolite membranes: M1 (a and b) and M2 (c and d) (operating conditions: T=400°C, R_{H_2O}=1.25, GHSV=1800 L_N kg_{cat}^{-1} h^{-1}, F_{H_2O}=6.25 mL min^{-1}).

[Color figure can be viewed in the online issue, which is available at wileyonlinelibrary.com.]

significantly due to the dilution by steam. The reduced pressure drop of H_2 would lead to less amount of H_2 removal from the reaction system through the membrane. It can be also seen from the figure that the χ_{CO} in MR increased with the $R_{H_2O/CO}$, which was similar to PBR. It was found that the CO conversion for MR was very close to that for PBR at 400°C, while obvious increase in CO conversion for MR vs. PBR was achieved during the whole range of steam to CO feed ratio at 350°C. This was because the enhancement by MR was more significant when the CO conversion largely deviated from equilibrium conversion. We noted that the increment in CO conversion for MR vs. PBR decreased with the steam/CO ratio. Similar phenomenon was also found in our previous work.[18] Due to reduced H_2 removal, the WGS enhancement by MR was weakened accordingly. As shown in the figure, the P_{H_2} decreased gradually with the $R_{H_2O/CO}$. We speculated that H_2O had more affinities to CO_2 than H_2.[29] When the steam partial pressure in the feed side increased, more H_2O molecules would stay in the zeolite channels on the feed side, which could be helpful for CO_2 permeation. Thus, the H_2 selectivity as well as H_2 permeate purity decreased.

Grid-scale simulation

From Figures 6–11, it is clearly seen that the modeling results agree well with the experimental data, indicating high reliability of the parameters used in this model. We predicted the WGS reaction performance in a wide condition region based on the model calculation. Figure 10 presents a simulation result of the χ_{CO} as a function of two-dimensional parameters of temperature and feed pressure for M1 and M2. The χ_{CO} increased and tended to plateau as the feed pressure increased. It was interesting to find that the χ_{CO} for M2 turned to surpass that for M1 when the feed pressure was above 0.4 MPa and the temperature was below 340°C. This could be ascribed to more reactants permeating through M1 with low selectivity under such high feed pressures, indicating that high quality membrane is crucial to high CO conversion in the MR under high feed pressure. The highest χ_{CO} for M1 and M2 were achieved to 88 and 92.2%, respectively, at 300°C under a feed pressure of 2 MPa.

To achieve high reaction efficiency, it is of great importance to optimize the membrane area matching with catalyst load. Figure 11 demonstrates the calculated χ_{CO} for M1 as a function of membrane length and catalyst load under feed pressures of 0.1 and 1 MPa, respectively. It is well known that large catalyst load favors high CO conversion. As shown in the figure, when operated under low pressure, the χ_{CO} increased dramatically as the catalyst load increased from 0.1 to 0.5 g, where the conversion was determined by the kinetic rate. The χ_{CO} tended to plateau when further increase catalyst load, indicating an equilibrium state achieved. The χ_{CO} increased slightly when the membrane length was prolonged due to more H_2 removed. By contrast, when operated under high pressure of 1 MPa, the χ_{CO} even decreased slightly with the membrane length. This phenomenon could be attributed to that the amount of unreacted reactants permeating from the reaction system was considerable at high feed pressure.

Long-term stability of membrane reaction

In our previous work,[17] we demonstrated that the modified hollow fiber MFI zeolite membranes exhibited excellent stability in the separation of H_2/CO_2 containing steam and H_2S atmospheres. Here, we evaluated the long-term stability of the modified MFI zeolite membrane used in WGS reaction swept by steam. The permeate H_2, CO and CO_2 flow rates were tested at 400°C and $R_{H_2O/CO}$=1.25 under GHSV=1800 $L_N\ g_{cat}^{-1}h^{-1}$. It can been seen from Figure 12 that the permeate gas fluxes varied very slightly during one hundred hours reaction in despite of the membrane quality, indicating that the modified MFI zeolite membranes could generate a high-purity and stable H_2 permeate product which was not affected by sweeping steam during the WGS reaction. The χ_{CO} and R_{H_2} for both membranes were stable as well during the whole operation. M1 maintained a χ_{CO} of ~72% and R_{H_2} of ~6% while M2 had steady values of ~71% and ~4%. For other reported hydrogen-selective membranes, Pd alloy membranes have been evaluated to be good stability in HT-WGS reaction but insufficient in high CO content or trace H_2S atmospheres.[30] Silica membranes have exhibited stable H_2/CO_2 separation performance at HT but there has been few result about their long-term continuous reaction stability under HT-WGS system containing high content of vapor.[9,31–34] Up to now, we have not yet found any other report on the WGS MR which was conducted using steam as sweep gas to acquire high-purity H_2 product. So we believe it is great potential for MFI zeolite membrane to be applied in pure H_2 production in the future.

Conclusions

Hollow fiber type MFI zeolite membranes were modified with CCD of MDES to enhance H_2 permselectivity over CO_2 and then carried out in HT-WGS reaction. We have demonstrated that a significant increment in CO conversion and high H_2 permeate purity was achieved in MR using steam as sweep gas. A high conversion of 73.6% was obtained in MR at 350°C, which was higher than that in PBR (63.4%). Meanwhile the H_2 permeate purity was 98.2%. The H_2 permeate purity was found high on the membrane with better H_2 separation performance and under conditions of low sweep steam flow rate, feed pressure and steam-to-CO. Based on the modeling results, it is possible to achieve a high conversion in MR under the optimum condition. The modified hollow fiber MFI zeolite membrane showed about 100 h long-term stability during WGS reaction. The challenge for the modified hollow fiber MFI zeolite membrane was its relatively low H_2 permeance, which could be overcome by increasing the packing density. We also attempted to prepare hydrogen-selective MFI zeolite membrane on high-strength hollow fiber supports to enhance mechanical property of the membrane, which is ongoing in our lab. In a word, it is great potential for hollow fiber hydrogen-selective MFI zeolite membranes to be applied in pure hydrogen generation via WGS reaction.

Acknowledgments

This work is sponsored by National Natural Science Foundation of China (21490585, 21222602, and 21176117), the Key Project of Chinese Ministry of Education (No. 212060), the Outstanding Young Fund of Jiangsu Province (BK2012040), The "Six Top Talents" and "333 Talent Project" of Jiangsu Province, the Natural Science Foundation of the Jiangsu Higher Education Institutions of China (09KJA530002) and the Project Funded by the Priority Academic Program Development of Jiangsu Higher Education Institutions (PAPD).

Literature Cited

1. Lee JY, Lee DW, Lee KY, Wang Y. Cr-free Fe-based metal oxide catalysts for high temperature water gas shift reaction of fuel processor using LPG. *Catal Today*. 2009;146:260–264.
2. Mendes D, Garcia H, Silva VB, Mendes A, Madeira LM. Comparison of nanosized gold-based and copper-based catalysts for the low-temperature water−gas shift reaction. *Ind Eng Chem Res*. 2009; 48: 430–439.
3. Mendes D, Chibante V, Zheng JM, Tosti S, Borgognoni F, Mendes A, Madeira LM. Enhancing the production of hydrogen via water–gas shift reaction using Pd-based membrane reactors. *Int J Hydrogen Energy*. 2010;35:12596–12608.
4. Bi Y, Xu H, Li W, Goldbach A. Water–gas shift reaction in a Pd membrane reactor over Pt/Ce0.6Zr0.4O2 catalyst. *Int J Hydrogen Energy*. 2009;34:2965–2971.
5. Barbieri G, Brunetti A, Tricoli G, Drioli E. An innovative configuration of a Pd-based membrane reactor for the production of pure hydrogen. *J Power Sources*. 2008;182:160–167.
6. Battersby S, Duke M C, Liu S, Rudolph V, Diniz da Costa JC. Metal doped silica membrane reactor: operational effects of reaction and permeation for the water gas shift reaction. *J Membr Sci*. 2008; 316:46–52.
7. Giessler S, Jordan L, Diniz da Costa JC, Lu GQ. Performance of hydrophobic and hydrophilic silica membrane reactors for the water gas shift reaction. *Sep Purif Technol*. 2003;32:255–264.
8. Qi H, Chen H, Li L, Zhu G, Xu N. Effect of Nb content on hydrothermal stability of a novel ethylene-bridged silsesquioxane molecular sieving membrane for H2/CO2 separation. *J Membr Sci*. 2012; 421–422:190–200.
9. Battersby S, Smart S, Ladewig B, Liu S, Duke MC, Rudolph V, Diniz da Costa JC. Hydrothermal stability of cobalt silica membranes in a water gas shift membrane reactor. *Sep Purif Technol*. 2009;66:299–305.
10. Masuda T, Fukumoto N, Kitamura M, Mukai SR, Hashimoto K, Tanaka T, Funabiki T. Modification of pore size of MFI-type zeolite by catalytic cracking of silane and application to preparation of H2-separating zeolite membrane. *Microporous Mesoporous Mater*. 2001; 48:239–245.
11. Gu X, Tang Z, Dong J. On-stream modification of MFI zeolite membranes for enhancing hydrogen separation at high temperature. *Microporous Mesoporous Mater*. 2008;111:441–448.
12. Tang Z, Dong J, Nenoff TM. Internal surface modification of MFI-type zeolite membranes for high selectivity and high flux for hydrogen. *Langmuir*. 2009;25:4848–4852.
13. Zhu X, Wang H, Lin YS. Effect of the membrane quality on gas permeation and chemical vapor deposition modification of MFI-type zeolite membranes. *Ind Eng Chem Res*. 2010;49:10026–10033.
14. Wang H, Lin YS. Effects of synthesis conditions on MFI zeolite membrane quality and catalytic cracking deposition modification results. *Microporous Mesoporous Mater*. 2011;142:481–488.
15. Wang H, Lin YS. Synthesis and modification of ZSM-5/silicalite bilayer membrane with improved hydrogen separation performance. *J Membr Sci*. 2012;396:128–137.
16. Hong Z, Wu Z, Zhang Y, Gu X. Catalytic cracking deposition of methyldiethoxysilane for modification of zeolitic pores in MFI/α-Al2O3 zeolite membrane with H+ ion exchange pretreatment. *Ind Eng Chem Res*. 2013;52(36):13113–13119.
17. Hong Z, Sun F, Chen D, Zhang C, Gu X, Xu N. Improvement of hydrogen-separating performance by on-stream catalytic cracking of silane over hollow fiber MFI zeolite membrane. *Int J Hydrogen Energy*. 2013;38:8409–8414.
18. Zhang Y, Wu Z, Hong Z, Gu X, Xu N. Hydrogen-selective zeolite membrane reactor for low temperature water gas shift reaction. *Chem Eng J*. 2012;197:314–321.
19. Kanezashi M, Lin YS. Gas permeation and diffusion characteristics of MFI-type zeolite membranes at high temperatures. *J Phys Chem C*. 2009;113:3767–3774.
20. Bustamante F, Enick RM, Cugini AV, Killmeyer RP, Howard BH, Rothenberger KS, Ciocco MV, Morreale BD, Chattopadhyay S, Shi S. High-temperature kinetics of the homogeneous reverse water-gas shift reaction. *AIChE J*. 2004;50:1028–1041.

21. Hla S, Park D, Duffy G, Edwards J, Roberts D, Ilyushechkin A, Morpeth L, Nguyen T. Kinetics of high-temperature water-gas shift reaction over two iron-based commercial catalysts using simulated coal-derived syngases. *Chem Eng J*. 2009;146:148–154.
22. Kim S-J, Yang S, Reddy GK, Smirniotis P, Dong J. Zeolite membrane reactor for high-temperature water-gas shift reaction: effects of membrane properties and operating conditions. *Energy Fuels*. 2013; 27:4471–4480.
23. Tang Z, Kim S J, Reddy G K, Dong J, Smirniotis P. Modified zeolite membrane reactor for high temperature water gas shift reaction. *J Membr Sci*. 2010;354:114–122.
24. Wang H, Lin Y S. Effects of water vapor on gas permeation and separation properties of MFI zeolite membranes at high temperatures. *AIChE J*. 2012;58:153–162.
25. Kanezashi M, O'Brien-Abraham J, Lin YS, Suzuki K. Gas permeation through DDR-type zeolite membranes at high temperatures. *AIChE J*. 2008;54:1478–1486.
26. Brunetti A, Barbieri G, Drioli E, Lee KH, Sea B, Lee DW. WGS reaction in a membrane reactor using a porous stainless steel supported silica membrane. *Chem Eng Process: Process Intensification*. 2007; 46:119–126.
27. Smart S, Venteb JF, Diniz da Costa JC. High temperature H2/CO2 separation using cobalt oxide silica membranes. *Int J Hydrogen Energy*. 2012;37:12700–12707.
28. Kim SJ, Xu Z, Reddy GK, Smirniotis P, Dong J. Effect of pressure on high-temperature water gas shift reaction in microporous zeolite membrane reactor. *Ind Eng Chem Res*. 2012;51: 1364–1375.
29. Gu X, Dong J, Nenoff TM. Synthesis of defect-free FAU-type zeolite membranes and separation for dry and moist CO2/N2 mixtures. *Ind Eng Chem Res*. 2005;44:937–944.
30. Augustine AS, Mardilovich IP, Kazantzis NK, Hua MY. Durability of PSS-supported Pd-membranes under mixed gas and water–gas shift conditions. *J Membr Sci*. 2012;415–416:213–220.
31. Uhlmann D, Smart S, Diniz da Costa JC. H2S stability and separation performance of cobalt oxide silica membranes. *J Membr Sci*. 2011;380:48–54.
32. Yacou C, Smart S, Diniz da Costa JC. Long term performance cobalt oxide silica membrane module for high temperature H2 separation. *Energy Environ Sci*. 2012;5:5820.
33. Smart S, Lin CXC, Ding L, Thambimuthu K, Diniz da Costa JC. Ceramic membranes for gas processing in coal gasification. *Energy Environ Sci*. 2010;3:268–278.
34. Wang H, Dong X, Lin YS. Highly stable bilayer MFI zeolite membranes for high temperature hydrogen separation. *J Membr Sci*. 2014;450:425–432.

Manuscript received Dec. 8, 2014, and revision received May 17, 2015.